Photofission of ^{238}U with monochromatic gamma rays in the energy range 11–16 MeV

W. Wilke, U. Kneissl, and Th. Weber

Institut für Kernphysik, Strahlenzentrum Justus-Liebig-Universität Giessen, Giessen, Germany

H. Ströher

Gesellschaft für Schwerionenforschung, Darmstadt, Germany

L. S. Cardman, P. T. Debevec, S. D. Hoblit,[*] R. T. Jones, and A. M. Nathan

Nuclear Physics Laboratory and Department of Physics University of Illinois at Urbana–Champaign, Champaign, Illinois 61820

We have measured the angular and mass distributions of the fragments from photofission of ^{238}U using tagged photons with energies between 11 and 16 MeV. The fission fragments were detected by a 4π arrangement of position-sensitive parallel-plate avalanche counters. Anisotropic angular distributions have been observed for the first time in the energy range where second-chance fission becomes energetically possible. A consistent assignment of J^{π} and K for the fission channels in ^{237}U has been deduced from a combined analysis of (γ, nf) and $(e, e'f)$ data. A clear relationship between the anisotropies and the fragment mass asymmetry has also been established. This correlation, together with the energy dependence of the angular distribution parameters, points to a possible interpretation of the results in terms of a recent theoretical model incorporating multiple exit channels in fission.

I. INTRODUCTION

Experiments with real photons represent an important tool for the investigation of the nuclear fission process. The measurement of fragment angular distributions at excitation energies near the fission barriers reveals information on the spectrum of transition states, which, in turn, is directly related to the shape of the nucleus at the saddle-point deformation. In addition, the properties of the fissioning system as it progresses from the outer saddle of the potential energy surface to the scission point can be studied by measuring the mass and energy distributions of the fragments.

Due to the lack of intense sources of monoenergetic photons, most systematic studies[1-4] of photofission-fragment angular correlations performed to date have used the continuous photon spectrum obtained from electron bremsstrahlung. As a consequence unfolding procedures had to be applied to extract the angular correlation coefficients as a function of the excitation energy. A few photofission experiments have been performed using monochromatic photons with very good energy resolution obtained from (n, γ)[5,6] and (p, γ)[7-10] reactions. Important results have been obtained from these experiments with a great deal of effort, but the experiments suffered from the fact that these photon sources lack a wide range of energies.

Recently photofission experiments using monoenergetic, tagged photons have become feasible because of the development of a new generation of electron ac-

celerators having high duty factors. Measurements of the photofission cross section using tagged photons have demonstrated the feasibility of this technique even at low photon energies.[11] A tagged photon experiment with very good energy resolution (≈ 18 keV) revealed structures in the cross section for energies around the fission barrier of ^{232}Th and ^{238}U,[12] which cannot be explained by the smooth absorption cross section.[13] It is of great interest to determine the quantum numbers of these resonances in the cross sections of actinide nuclei by measuring the fragment angular distributions. Unfortunately, the cross section near threshold is very small (a few mb) so a large amount of beam time is required for measurements of angular distributions, which need excellent statistics. In the energy range of the second-chance fission threshold, B_{nf}, the cross sections are significantly higher. Therefore, one motivation for the present experiment was to take advantage of the higher cross section in this region to investigate the angular distributions of fission fragments from ^{238}U after neutron-evaporation in order to obtain information on the low-lying transition states in ^{237}U. It is also worth mentioning that target nuclei that are unstable become accessible by studying fission at the second chance fission threshold (^{237}U in the case of the present experiment).

The present investigation was also stimulated by very recent results from a photofission experiment performed at Giessen.[14] That experiment, which used continuous (untagged) bremsstrahlung, found a correlation between the quantum numbers of the transition states and the

fragment mass asymmetry for ^{236}U. In the present ex-
periment we performed a simultaneous measurement of
both the angular and mass distributions of the fragments
to investigate a possible dependence of the fragment mass
ratio on the quantum numbers of the transition states.
^{238}U has been chosen as a target because a compari-
son with recent ^{238}U$(e, e'f)$ data[15,16] and ^{239}Pu(γ, f)
experiments[17] should help establish consistent assign-
ments for the quantum numbers of the transition states
in ^{237}U. The Pu experiment is relevant because the nu-
cleus ^{239}Pu has the same ground state spin, $J_0^\pi = \frac{1}{2}^+$, as
^{237}U.

II. EXPERIMENTAL APPARATUS

The experiment was performed using the tagged pho-
ton facility at the Nuclear Physics Laboratory of the Uni-
versity of Illinois.[18] A cw electron beam with an energy
E_0=21 MeV and an energy spread $\Delta E_0/E_0$=10^{-3} was
obtained from the superconducting microtron MUSL-
2.[18] Monoenergetic tagged photons were produced by
the bremsstrahlung monochromator method.[19] The mag-
netic spectrometer possesses a total momentum accep-
tance of p_{max}/p_{min}=1.5; it was adjusted to provide
tagged photons in the energy range $(0.57 \pm 0.08)E_0$ and
$(0.81 \pm 0.04)E_0$ (with photon energy resolutions of 0.9%
and 0.3%, respectively). Two settings of the magnetic
field of the spectrometer were used to produce photons
with energies between 11 and 16 MeV with an energy res-
olution of 80–120 keV for each of the 32 electron channels.
Electron beam currents of several tens of nanoamperes
were delivered, resulting in some 10^6 photons per second
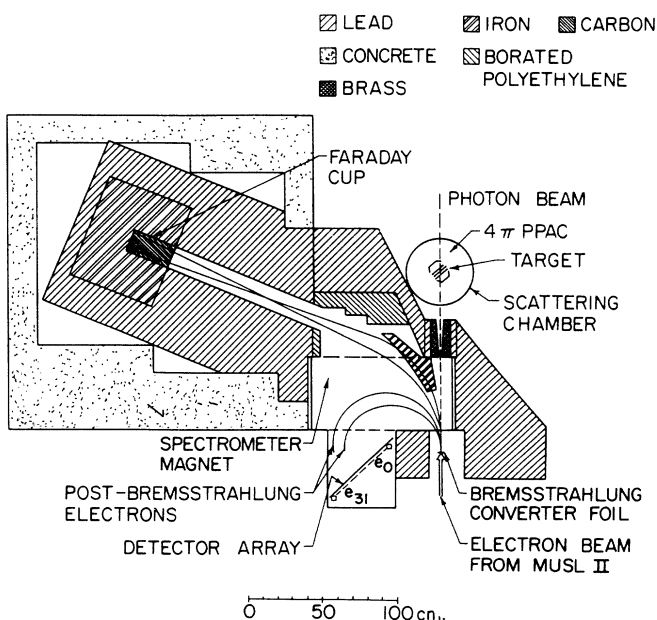per energy bin when using a 25-μm aluminum radiator.
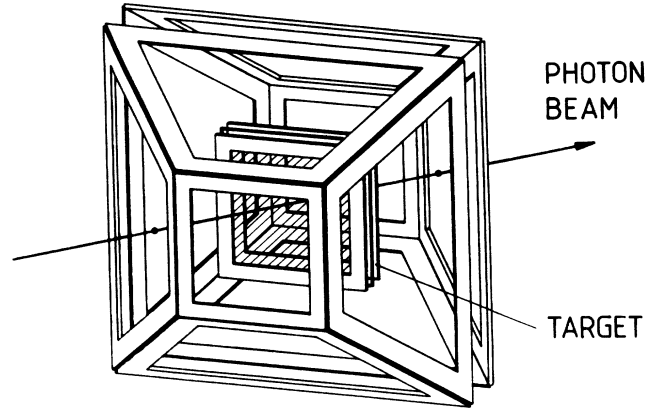

FIG. 2.   Schematic drawing of the 4π PPAC arrangement.

The experimental facility is shown schematically in
Fig. 1. The distance between the radiator and the fission
target was approximately 1.25 m. With a conical colli-
mator $(\phi_1$=4.75 cm, ϕ_2=5.75 cm) a photon beam spot
of 7 cm diameter was obtained at the target position. A
homogeneous 7 cm×10 cm fissile target of 400μg/cm^2 of
^{238}U evaporated onto a 200μg/cm^2 mylar foil was used.
This target is sufficiently thin that both complementary
fragments could emerge and be detected.

A dedicated 4π arrangement of 12 position-sensitive
parallel-plate avalanche counters (PPAC's) was built in
order to measure the photofission fragment angular and
mass distributions simultaneously (see Fig. 2). This de-
tector system, which was constructed at Giessen, is de-
scribed in more detail elsewhere.[20] The target was sand-
wiched between the two inner detectors, which are sepa-
rated by a distance of 1 cm. These two detectors provided
spatial information as well as the start signals for the
double time-of-flight (TOF) measurement, which permit-
ted the fragment mass information to be deduced. The
angle of the target and the normal vector of the detec-
tor plane relative to the photon beam direction was 45°.
The target-detector sandwich was also used as an on-
line beam position and profile monitor.[21] We corrected
the data event-by-event for the angular divergence of the
tagged photon beam and the large spot size at the tar-
get position by reconstructing the origin of each fission
event on the target. Two hemispheres, each consisting of
five independent detectors, were mounted a distance of
12.5 cm from the target center, and covered a solid angle
of almost 4π. These detectors provided a second mea-
surement of the position of each fragment, permitting
the reconstruction of its trajectory; they also provided
the stop signals for the double TOF measurements. The
velocities of both fragments were determined from the
known flight paths and measured TOF's. The fragment
mass distributions were deduced by a conventional anal-
ysis using momentum and mass conservation. To obtain
reliable fragment mass distributions it was necessary to
correct the data on an event-by-event basis for the ef-

LEAD   IRON   CARBON
CONCRETE   BORATED
BRASS   POLYETHYLENE

FARADAY CUP

PHOTON BEAM

4 π PPAC

TARGET

SCATTERING CHAMBER

SPECTROMETER MAGNET

POST-BREMSSTRAHLUNG ELECTRONS

DETECTOR ARRAY

BREMSSTRAHLUNG CONVERTER FOIL

ELECTRON BEAM FROM MUSL II

0   50   100 cn.

FIG. 1.   The University of Illinois tagging facility and the
experimental setup.

fects of energy loss in the target, in the cathode foils of the inner detectors, and in the counter gas.[20] The overall mass resolution of $\Delta m \leq 5$ amu achieved by this procedure was sufficient for the objectives of the present experiment. This arrangement of low pressure proportional counters was operated in a vacuum chamber completely filled with isobutane at a pressure of 4.3 mbar.

The characteristics of the response of the PPAC detector system were determined in a separate measurement at the beginning of the experiment that used a high-intensity, untagged bremsstrahlung beam from a thick (1 mm) tungsten radiator, but left the experimental apparatus (geometry, thresholds, etc.) unchanged. This measurement provided the data needed for the normalization of the angular distributions by revealing the solid angle and efficiency of each fission detector. The differences in the detector's response for different fragment masses due to different thresholds and due to absorption effects in the target, the target backing, and the detector windows were fully accounted for by this experimental procedure.

III. PHOTOFISSION CROSS SECTIONS

The absolute photofission cross section in a tagged photon experiment is given by[22]

$$\sigma_{\gamma,f}(E_\gamma) = \frac{N_{ft}(E_\gamma)}{N_e(E_\gamma)} \frac{1}{\varepsilon(E_\gamma)} \frac{1}{\varepsilon_f \Omega_f t} \frac{A_m}{N_A}. \quad (1)$$

To obtain the cross section the following experimental quantities have to be determined: (i) the tagging efficiency ε, which is the ratio of tagged photons $N_{\gamma c}$ to electrons N_e in the corresponding energy bin; (ii) the number of true fission events N_{ft}; (iii) the product $\varepsilon_f \Omega_f$ of the efficiency and the solid angle of the fission detector; and (iv) the effective target thickness t. A_m is the mass number of the target and N_A is Avogadro's number.

The tagging efficiency was measured in separate calibration runs with a 25.4 cm × 35.6 cm NaI detector using a very low intensity electron beam (pA) with an endpoint energy of 21 MeV to produce the tagged photons. ε was rather constant for low photon energies ($\approx 45\%$ at $E_\gamma = 11$ MeV and $\approx 40\%$ at $E_\gamma = 14$ MeV), but a steeper decrease was obtained for higher photon energies ($\approx 15\%$ at $E_\gamma = 16$ MeV). After subtraction of the accidental coincidences, more than 10^3 true fission events, N_{ft}, were accumulated for each energy bin for both magnetic field settings. $\varepsilon_f \Omega_f$ was determined by matching the angle-integrated cross sections from this experiment to the absolute cross sections measured at Saclay.[23] From this comparison a value of $\varepsilon_f \Omega_f = 0.55$ was deduced, which is reasonable in view of the fact that the detector efficiency is close to unity and slightly more than half of the 4π solid angle is covered by the active area of the detector.

Figure 3 shows the results of this experiment for the angle-integrated (γ, f) cross section. The normalized cross sections agree fairly well with the shape of the absolute cross section data measured by the Saclay group[23]
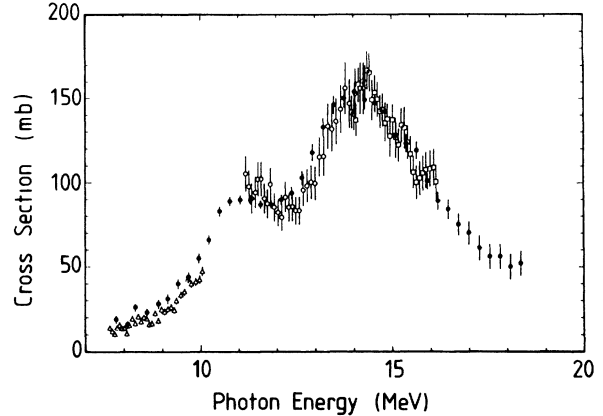

FIG. 3. Photofission cross section for ^{238}U. The open symbols ($\triangle$, o, $\square$) correspond to the present experiment (different runs), and the full symbols ($\bullet$) are the Saclay data.[23]

using quasimonoenergetic photons from positron annihilation in flight, although our data exhibit a slight shift to higher energies. This shift is not seen if our cross sections are compared with the results of an $(e, e'f)$ experiment on ^{238}U which had an energy resolution of 40 keV.[15] The absolute scale of the photon energy in the present experiment has only been determined with an accuracy of 200 keV, whereas a resolution per energy interval of 80–100 keV was achieved. This agreement indicates the reliable operation of the experimental apparatus. Other data sets[22,24] reported in the literature show the same energy dependence.

IV. ANGULAR DISTRIBUTIONS

To evaluate the total cross section from these data, the number of true fission events was obtained by subtracting the accidental coincidences from the total coincidences using appropriate windows in the coincidence time spectrum. In order to determine the angular distributions of fission fragments in a tagged photon experiment, a more sophisticated analysis was applied. In the upper part of Fig. 4, a coincidence time spectrum between the fission detector and one of the electron detectors is shown. The contribution to the angular distributions of the accidental background in the peak region of the true fission events was taken into account by determining the angular distributions in appropriate windows to the left and right of the peak position.

The angular distributions for the various regions of the coincidence time spectrum were normalized using the measured response function of the fission detector. It was observed that the accidental events outside the peak region exhibit an isotropic angular distribution for all data samples; a typical example is shown in Fig. 4(b). The accidental coincidence background is expected to be isotropic because the accidental fission-fragment spectrum is dominated by events coming from the untagged
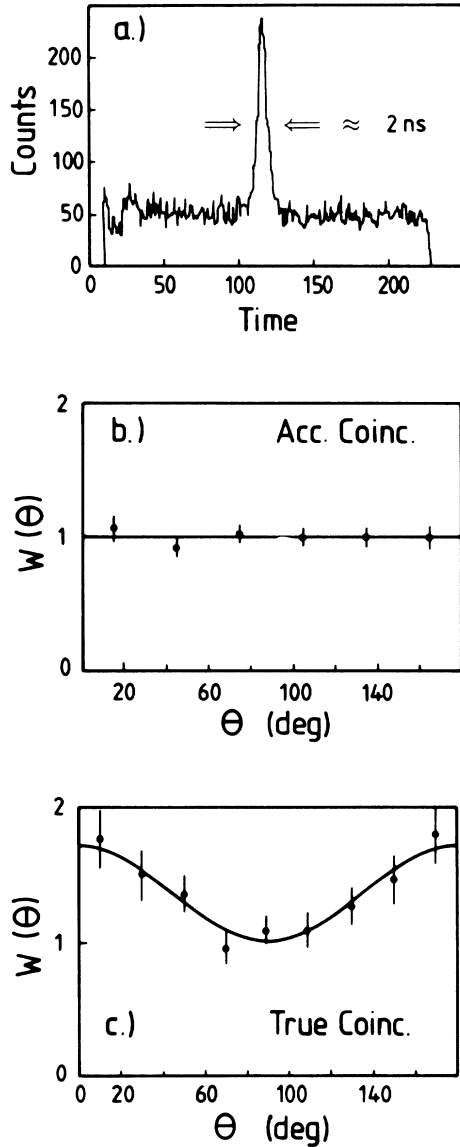
FIG. 4. Experimental spectra for (E_γ=11.3 MeV): (a) a time spectrum of coincidences (resolution FWHM $\approx$2 ns); (b) the fragment angular distribution for accidental coincidences; and (c) the fragment angular distribution for true coincidences.

FIG. 5. The angular correlation coefficient b as a function of the photon energy: (a) integrated over all masses; (b) for a "quasisymmetric" mass split; and (c) for a "far-asymmetric" mass split.

portion of the bremsstrahlung spectrum. Therefore, it can be expected to have an angular distribution similar to that obtained in measurements using a continuous (untagged) bremsstrahlung beam. These distributions have been observed[3,25] to be isotropic for sufficiently high beam energies (including the value of $E_0 = 21$ MeV used for the present experiment). All nonfission events such as α-particles are strongly suppressed by the requirement of a coincidence between the two inner and the two outer fission detectors, so only fission fragments contribute to the accidentals spectrum.

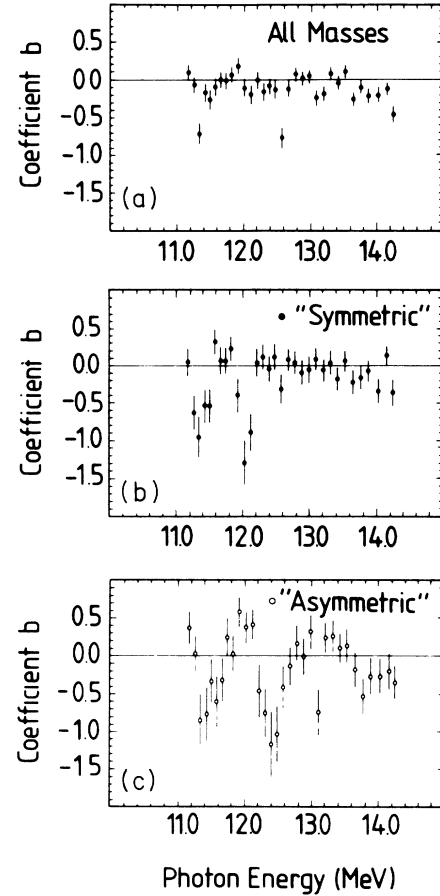The angular distributions of the true events are de-

termined by correcting for the accidental coincidences in the peak region. An example is shown in Fig. 4(c) for E_γ $\approx$11.3 MeV, where a large anisotropy is evident. Due to the limited number of true fission events, an angular bin size of 20° was chosen. The solid line in the figure represents a least-squares fit to the experimental data, employing the usual parametrization:[26]

$$W(\theta) = a + b\sin^2\theta + c\sin^2 2\theta. \tag{2}$$

This is the general form used to describe the angular distribution of photofission fragments in the case of dipole and quadrupole excitation. No quadrupole contributions have been observed in the energy region investigated; the c coefficient in the fits to our data was always compatible with zero. The distributions were normalized in such a way that $a + b = 1$, where a corresponds to the isotropic portion and b is proportional to the anisotropy, A, as can be seen from the ratio of the angular correlation coefficients:

$$\frac{b}{a} = \frac{W(90°)}{W(0°)} = A - 1. \tag{3}$$

Figure 5(a) summarizes the b values deduced from the

angular correlations as a function of the photon energy in the region of the second chance fission threshold B_{nf}. The error bars shown were obtained from the least-squares procedure. In the energy range shown the angular distribution is isotropic ($b=0$) except for two energies, $E_\gamma \approx 11.3$ MeV and $E_\gamma \approx 12.6$ MeV, where large negative b values appear. This is the first time that large anisotropies have been observed in a photofission experiment for such high photon energies.

The angular distributions of the fission fragments have also been analyzed for particular mass splits in the fragment mass distributions, which were measured simultaneously using the double time-of-flight method. The fragment mass distribution for ^{238}U(γ, f) obtained in the

FIG. 6. The mass distribution for ^{238}U (γ, f) obtained using bremsstrahlung with an endpoint energy $E_0 = 21$ MeV (a); and the fragment angular distributions at $E_\gamma = 12.13$ MeV for a "quasisymmetric" mass split (b), and a "far-asymmetric" mass split (c).

run using bremsstrahlung with an end-point energy of 21 MeV is shown in the upper part of Fig. 6; larger symmetric contributions are observed at this energy than is the case for the photon energy range of 11–16 MeV. The shaded regions in this figure indicate the mass cuts used to define "symmetric" and "asymmetric" fission. Since the mass distribution is continuous, these cuts are somewhat arbitrary; we define symmetric fission as fission in which the ratio of the fragment masses is between 1 and 1.2, and asymmetric fission as fission in which this ratio is greater than 1.75. For a photon energy of 12.13 MeV these mass splits result in two very different angular distributions, plotted in the lower part of Fig. 6. This corroborates the results of an earlier experiment performed at Giessen using continuous bremsstrahlung,[14] in which a correlation between the quantum numbers of transition states and the fragment mass asymmetry in the near barrier photofission of ^{236}U was found. In addition there is a pronounced energy dependence. This can be seen from Figs. 5(b) and (c), where the angular correlation coefficients b for these mass splits are plotted versus photon energy. For both mass regions considered two large anisotropies have been observed. These mass-selected anisotropies are similar to those observed without selection of the mass ratios [Fig. 5(a)] but a broadening in energy is seen in all of the mass-selected anisotropies, and energy shifts are observed for the higher energy anisotropy. The asymmetry at 12.6 MeV in the total fission angular distribution occurs at a lower energy in the mass-selected anisotropies, and the symmetric fission anisotropy has shifted further than the asymmetric anisotropy. In contrast, the asymmetry observed at lower energy ($\sim$11.3 MeV) occurs at the same energy for both the total fission and the mass-selected fission angular distributions.

V. DISCUSSION

First-chance photon-induced fission of the nucleus ^{238}U cannot explain the large anisotropies observed in the angular distributions near the B_{nf} threshold because the large number of different fission channels energetically available at this excitation energy would result in isotropic distributions.[26] In particular, it seems to be unreasonable to connect the observed anisotropies with first-chance fission of the $K=1$ part of the giant electric dipole resonance (GDR). The GDR has a width $\Gamma \approx 5$ MeV, and is located at an excitation energy of about 5 MeV above the fission barrier of ^{238}U, a region of a very high level density. The fission decay of these continuum states should not lead to an anisotropic emission of the fragments in a rather narrow energy range. Therefore, one has to consider second-chance fission, i.e., fission after the evaporation of a neutron, to explain the anisotropies observed in this experiment. In the case of second-chance fission, the fragments originate from the low energy fission of ^{237}U, which has a ground state spin and parity of $J^\pi = \frac{1}{2}^+$.
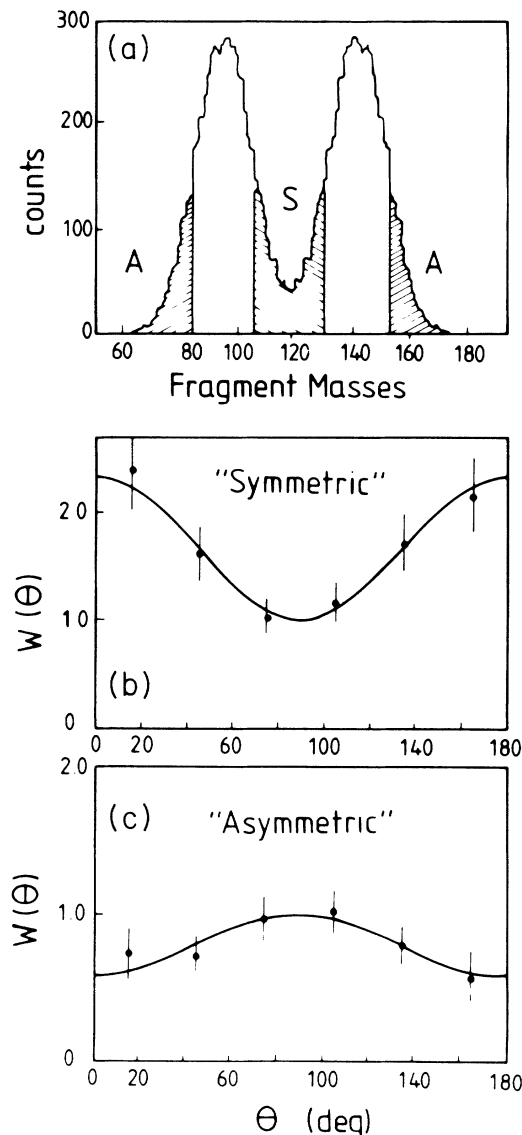
As will be shown below, the comparison of (γ, f) and $(e, e'f)$ experiments on ^{238}U represents a powerful method for obtaining a consistent assignment of quantum numbers for the transition states in ^{237}U, since virtual and real photons excite different magnetic substate populations in ^{238}U, leading to different angular correlations. The excitation mechanism is shown schematically in Fig. 7, where pure electric dipole excitation of the ^{238}U target nuclei is assumed. In the figure K denotes the component of the total angular momentum J of the compound nucleus ^{237}U along the nuclear symmetry axis, while M is the projection of the total angular momentum on the direction of the momentum transfer q (for real photons given by the beam axis) (see inset of Fig. 7). For the nucleus ^{238}U these projections are denoted χ and μ, respectively. In $(e, e'f)$ and $(e, e'nf)$ reactions at modest momentum transfers and forward scattering angles the excitation is dominantly longitudinal, i.e., $\mu=0$; in (γ, f) and (γ, nf) reactions the excitation is purely transverse, i.e., $\mu = \pm 1$. $E1$ excitation of ^{238}U leads to states with quantum numbers $\chi = 0, \pm 1$.

Based on the transmission coefficients for neutron evaporation,[27] we expect only s- and p-wave neutrons to contribute significantly to the formation of the compound nucleus ^{237}U near the second-chance fission threshold. With this assumption only the states of the five different K bands shown in Fig. 7 can be excited. Starting
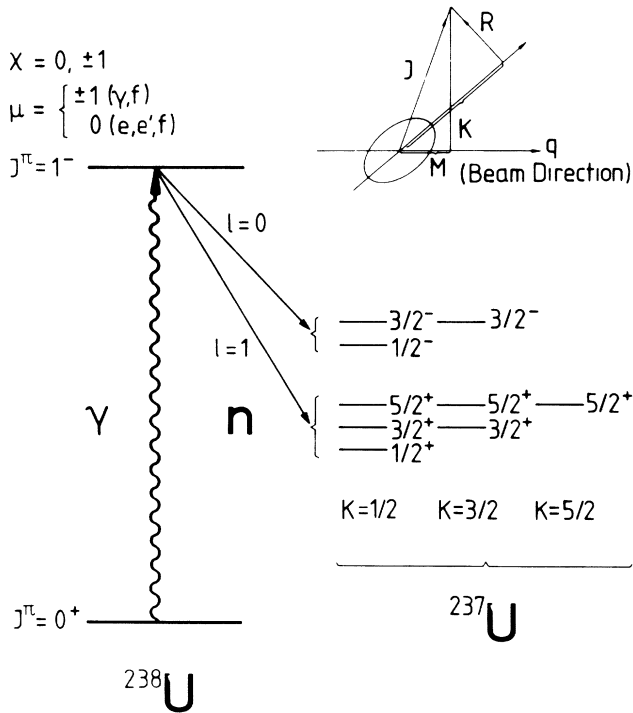
TABLE I. Anisotropies b/a of different K bands for ^{238}U(γ, nf) and ^{238}U$(e, e'nf)$

(J^π, K)	b/a $_{(\gamma, nf)}$	$b/a_{(e, e'nf)}$
$\leq \frac{3}{2}^-, \frac{1}{2}$ [a]	0.75	-0.50
$\frac{3}{2}^-, \frac{3}{2}$ [a]	-0.50	$(b = 1.0, \ a = 0)$
$\leq \frac{5}{2}^+, \frac{1}{2}$ [b]	$0.10 \cdots 0.23$	$-0.08 \cdots -0.25$
$\leq \frac{5}{2}^+, \frac{3}{2}$ [b]	$0.12 \cdots 0.20$	$-0.33 \cdots -0.39$
$\frac{5}{2}^+, \frac{5}{2}$ [a]	-0.50	$(b = 1.5, \ a = 0)$

[a] Result independent of transmission coefficients.
[b] Results for different transmission coefficients and neutron energies of $E_n=200$ and 400 keV, respectively.

from 1^- states in ^{238}U, negative parity states and positive parity states are excited following s-wave $(l=0)$ and p-wave $(l=1)$ neutron neutron evaporation, respectively. The relative angular distributions for both processes were calculated by summing over the product of partial formation probabilities of the compound nucleus $P(j, JM)$ and the angular distribution functions $W(JMK, \theta)$ for fission fragments emitted from those compound states:[26]

$$W(\theta) \propto \sum_j \sum_J \sum_M P(j, JM) W(JMK, \theta). \qquad (4)$$

The summation in this equation was performed over all quantum numbers available; j is the total angular momentum of the emitted neutron. The transmission coefficients were deduced from optical model calculations.[27] In Table I the theoretical b/a values for the different K bands of Fig. 7 are listed for ^{238}U(γ, nf) and ^{238}U$(e, e'nf)$ in order to compare the predicted sign for the anisotropy. The level spacings of the states in a K band are small compared to the total energy resolution, which is due to the energy resolution of the photon beam and the energy spreading due to the neutron emission. Therefore, one must sum all of these contributions to the relative angular distributions. The ratio b/a is a measure for the anisotropy as it corresponds to the ratio $W(90°)/W(0°)$. Remembering that the angular correlation coefficient a gives the isotropic contribution to the cross section (i.e., $a \geq 0$), we note that the coefficient b will determine the sign of b/a.

The exclusive $(e, e'f)$ experiment for ^{238}U has been performed at the Mainz Microtron MAMI A $(E_e^{max}=185$ MeV$)$. The data were taken at different momentum transfers q, but here the discussion focuses on the results for $q_{eff}=0.20$ fm^{-1}; at this q value $E1$ excitations are predominant. The experiment revealed a positive anisotropy, $b/a=+(0.56\pm0.20)$, for excitation energies $\omega = E_\gamma \approx 12.3$ MeV, which is near to the B_{nf} threshold,[15,28] whereas negative b/a values are observed for real photons (see Fig. 5). These anisotropies most likely originate from fission after neutron evaporation from compound nuclear states of ^{237}U with $(J^\pi, K) = (\frac{3}{2}^-, \frac{3}{2})$ or $(\frac{5}{2}^+, \frac{5}{2})$, since their relative angular anisotropies exhibit the correct sign for both (γ, nf) and

FIG. 7. A schematic representation of the ^{238}U(γ, nf) and ^{238}U$(e, e'nf)$ reactions and possible populations of various bands in ^{237}U. The inset shows the coupling scheme of angular momenta in a deformed nucleus; J=the total angular momentum, R=the rotational angular momentum, K=the projection of J on the symmetry axis, and M=the projection of J on the quantization axis z (the beam direction).

$(e, e'nf)$ experiments.

There are also (γ, f) angular distribution data[17] available for ^{239}Pu, which has the same ground-state spin, $\frac{1}{2}^+$, as ^{237}U. This (γ, f) experiment was performed with continuous bremsstrahlung for energies near the fission barrier. No $J^\pi = \frac{5}{2}^+$ state contributions, which would be accessible by $E2$-absorption, were observed in this experiment; a dominant channel spin of $\frac{3}{2}^-$ was deduced. If the $\frac{3}{2}^-$ state were higher in energy than the $\frac{5}{2}^+$ state, there would be a large $E2$ contribution, especially for low photon energies, due to the increased penetrability through the lower $\frac{5}{2}^+$ fission barrier. This behavior has been observed[29] in the photofission of even-even nuclei near the fission threshold, where the $E2$ contributions in the fission channel are large compared to the $E1$ photoabsorption due to the relative heights of the 2^+ and 1^- barriers. The observation that no $J^\pi = \frac{5}{2}^+$ contributions therefore suggests that the $\frac{3}{2}^+$ state lies lower than the $\frac{5}{2}^+$ state in ^{239}Pu.

Based on these considerations, it seems reasonable to interpret our results in analogy with the observations in ^{239}Pu, i.e., that the $\frac{3}{2}^-$ state in ^{237}U is located at lower energies in the level scheme than the $\frac{5}{2}^+$ state in this nucleus. Following these arguments, it is possible to make a consistent identification of the states contributing to the tagged photon experiment by assuming that the anisotropy near 11.3 MeV is due to the $\frac{3}{2}^-$ state, while the anisotropy at the higher photon energy corresponds to the $\frac{5}{2}^+$ state.

The anisotropy observed at 11.3 MeV in the photofission data is not seen in the exclusive electron scattering experiment. This can be explained by the fact that virtual photons excite quadrupole states far more easily than real photons at these energies. Large quadrupole contributions occur in the $(e, e'f)$ reaction from the decay of the giant quadrupole resonance (GQR), which lies at an excitation energy $\omega \approx 8$–12 MeV. This $E2$ excitation leads to the superposition of a very different set of fission channels in $(e, e'f)$ than is the case in (γ, f); this, in turn, prevents the appearance of pronounced anisotropies in $(e, e'f)$. It should be noted that the experimental values for b/a [$+0.56\pm0.2$ for $(e, e'nf)$, -0.42 ± 0.1 and -0.44 ± 0.1 for (γ, nf)] are smaller than the theoretically predicted values. This can be explained by noting that a large fraction of fission products are coming from first-chance fission of ^{238}U, which is isotropic at these energies.

The fact that the $J^\pi = \frac{3}{2}^-$ state occurs at photon energies below the quoted B_{nf} threshold of 12.24 MeV for ^{238}U [calculated by adding the (γ, n) threshold in ^{238}U (6.14 MeV, Ref. 30) and the fission barrier of ^{237}U (6.1 $\pm$ 0.2 MeV), Ref. 31] may arise from the uncertainty[31] in the ^{237}U barrier heights since the neutron separation energies are known very precisely. As pointed out by Caldwell *et al.*,[24] the B_{nf} threshold should lie substantially lower in energy, which seems to be supported by

this experiment. The uncertainty in the absolute scale of the photon energy (≈ 200 keV) is too small to explain the difference between the calculated B_{nf} threshold and the location of the lower energy anisotropy. A large shift of the energy scale in the present experiment is prohibited by the excellent agreement between the energy dependence of the total photofission cross section measured in the present experiment and that of cross section data from a number of other laboratories for a variety of reactions. Fission probability data from a recent ^{236}U(d, pf) experiment[32] with very good energy resolution showed no resonancelike structures in the subbarrier energy region; the first resonances occur at 6.1–6.2 MeV excitation energy. These data are in agreement with fission probabilities deduced from the ^{236}U(n, f) cross section,[33] which seem to contradict the result of this experiment. However, the very different excitation mechanisms in (γ, f) and (n, f) might help explain this discrepancy, since the potential energy surface of the compound nucleus ^{237}U is not necessarily static and identical for different excitations leading to all of the fission reactions under consideration. To summarize, a variety of other experiments can be interpreted consistently with the present photofission data, and offer no compelling reason to question the energy scale of the present data.

No traditional model description like the static scission point model[34] or the two-component mode of fission[35] can explain our experimental findings. Recent dynamic descriptions like the multi-exit-channel fission model of Brosa *et al.*[36] seem to be more realistic, though no detailed calculations have been performed to date to explain the observed correlation between the quantum numbers of the transition states and the fragment mass division. The multi-exit-channel fission model describes the fragment mass, the average kinetic energy, and the variance distributions in thermal neutron-induced and spontaneous fission. For the light actinide nuclei (e.g., ^{236}U) one symmetric and two asymmetric channels are obtained; these are referred to as superlong, and standard I and II, respectively, and correspond to different nuclear shapes at the scission point. The corresponding fragment mass distributions and average total kinetic energies for these channels differ substantially. According to this model and the analysis of recent ^{235}U(n, f) experiments by Knitter *et al.*,[37] the contribution of the superlong (symmetric) channel should be small (<0.1 %) near the barrier. The standard I channel is centered around the mean mass $m = 134$ (18%), while the standard II channel dominates at masses $m \geq 140$.

For the photofission of ^{236}U it has been found[14] that the angular distributions are distinctly different if the mass splits in the analysis of the data are chosen to correspond to the above-mentioned mean masses of the standard I and II channels. Unfortunately, the statistical accuracy of the present data is not sufficient to select tighter mass splits for the quasisymmetric and far-asymmetric fission products. Therefore, the bounds chosen for the mass asymmetry analysis of the present data are some-

what arbitrary. Nevertheless, the results for the two fission channels deduced in ^{237}U around the B_{nf} threshold indicate a pronounced energy dependence for the coupling between standard I and II channels and the transition states. This might point to different nuclear shapes with respect to the quantum numbers of the contributing states, which differ in spin and parity. The results of a very recent ^{235}U(n, f) experiment near the fission threshold corroborates these experimental findings, since different angular distributions have also been observed for fission fragments of particular masses, which were separated by means of a radiochemical procedure.[38]

VI. CONCLUSIONS

The use of monoenergetic tagged photons enabled detailed photofission investigations in the energy range of the second chance fission threshold B_{nf} for the first time. The novel result of the present ^{238}U$(\gamma_{\text{tagged}}, nf)$ experiment is the observation of pronounced anisotropies in the fission fragment angular distributions at excitation energies near B_{nf} (≈ 12 MeV). The anisotropies can be explained qualitatively by near-barrier fission of the residual compound nucleus after neutron emission, ^{237}U. A comparison with recent ^{238}U$(e, e'f)$ data[28] and a previous ^{239}Pu(γ, f) experiment[17] (^{239}Pu has the same ground state spin of $\frac{1}{2}^{+}$ as ^{237}U) permits a spin and K-number assignment to two low-lying transition states in ^{237}U.

The fragment detector, a 4π PPAC arrangement,[20] enabled a simultaneous measurement of both the fragment mass and angular distributions. Much more pronounced anisotropies were observed for different mass regions (quasisymmetric and far-asymmetric mass splits, respectively). In addition, a shift in excitation energy

of the maximum of the anisotropies seems to be indicated. This complex energy dependence of the observed anisotropies for particular mass splits argues in favor of several complicated nuclear shapes for different fission paths as described within the framework of the recent multi-exit-channel fission model.[36] Such a correlation between the quantum numbers of the near barrier transition states (that determine the fragment angular distributions) and the mass split seems to be a rather general phenomenon. It has been observed recently in ^{236}U as well, both in photofission experiments[14] and in the ^{235}U(n_{therm}, f) reaction.[38] However, it should be noted that the relationship observed between the fragment angular and mass distributions is not simply a spin and parity effect. This is obvious from a comparison of mass distributions observed in the fission decay of various giant multipole resonances by recent $(e, e'f)$ coincidence experiments[39] and ^{236}U(γ, f) data.[14] This comparison provides evidence that the observed mass distributions depend strongly on the specific excitations leading to states of specific nuclear structure,[40] and are not simply dependent on the spins and parities of the excited compound states.

ACKNOWLEDGMENTS

*Present address: Physics Department, Brookhaven National Laboratory, Upton, New York, 11973.

[1] A. Alm and L. J. Lindgren, Nucl. Phys. A271, 1 (1976).

[2] L. J. Lindgren, A. Alm, and A. Sandell, Nucl. Phys. A298, 43 (1978).

[3] N. S. Rabotnov, G. N. Smirenkin, A. S. Soldatov, L. N. Usachev, S. P. Kapitza, and Yu. M. Tsipenyuk, Zh. Eksp. Teor. Fiz. 11, 508 (1970) [Sov. J. Nucl. Phys. 11, 285 (1970)].

[4] Yu. M. Tsipenyuk, Yu. B. Ostapenko, G. N. Smirenkin, and A. S. Soldatov, Usp. Fiz. Nauk. 144, 3 (1984) [Sov. Phys. Usp. 27, 649 (1984)].

[5] A. Manfredini, L. Fiore, C. Ramorino, H. G. de Carvalho, and W. Wölfli, Nucl. Phys. A123, 664 (1969); A127, 687 (1969).

[6] A. Manfredini, L. Fiore, C. Ramorino, and W. Wölfli, Nuovo Cim. A 4, 421 (1971).

[7] T. R. Yeh, and H. Lancman, IEEE, NS-28, 1289 (1981); Nucl. Instrum. Methods 179, 141 (1981).

[8] H. X. Zhang, T. R. Yeh, and H. Lancman, Nucl. Instrum. Methods 214, 391 (1983).

[9] H. X. Zhang, T. R. Yeh, and H. Lancman, Phys. Rev. Lett. 53, 34 (1984).

[10] H. X. Zhang, T. R. Yeh, and H. Lancman, Phys. Rev. C 34, 1397 (1986).

[11] P. A. Dickey and P. Axel, Phys. Rev. Lett. 35, 501 (1975).

[12] J. W. Knowles, W. F. Mills, R. N. King, B. O. Pich, S. Yen, R. Sobic, L. Watt, T. E. Drake, L. S. Cardman, and R. L. Gulbranson, Phys. Lett. 116B, 315 (1982); and (private communication).

[13] Y. Birenbaum, R. Alarcon, S. D. Hoblit, R. M. Laszewski, and A. M. Nathan, Phys. Rev C 35, 1293 (1987).

[14] W. Wilke, R. D. Heil, U. Kneissl, U. Seemann, F. Steiper, H. Ströher, and Th. Weber, Phys. Lett. B 207, 385 (1988).

[15] Th. Weber, R. D. Heil, U. Kneissl, W. Pecho, W. Wilke, H. J. Emrich, Th. Kihm, and K. T. Knöpfle, Phys. Rev. Lett. 59, 2028 (1987).

[16] Th. Weber, R. D. Heil, U. Kneissl, W. Wilke, H. J. Emrich, Th. Kihm, and K. T. Knöpfle, Phys. Lett. B 215, 469 (1988).

[17] A. S. Soldatov, Yu. M. Tsipenyuk, and G. N. Smirenkin, Zh. Eksp. Teor. Fiz. 11, 992 (1970) [Sov. J. Nucl. Phys. 11, 552 (1970)].

[18] Nuclear Physics Laboratory report, July (1980), University of Illinois, Urbana–Champaign, IL (unpublished).

[19] L. S. Cardman, Photon Tagging, Present Practice and Fu-

ture Prospects, Proceedings of the Magnetic Spectrometer Workshop, Williamsburg, VA, 1983; also available as Nuclear Physics Laboratory, University of Illinois, Urbana–Champaign, IL, Report No. P/83/12/168 (unpublished).

[20]W. Wilke, H. Brückel, R. Heil, U. Kneissl, H. Ströher, and Th. Weber, Nucl. Instrum. Methods A272, 785 (1988).

[21]W. Wilke, H. Brückel, R. Heil, U. Kneissl, H. J. Maier, K. Schaschek, H. Ströher, and Th. Weber, Nucl. Instrum. Methods A249, 544 (1986).

[22]H. Ries, U. Kneissl, G. Mank, H. Ströher, W. Wilke, R. Bergère, P. Bourgeois, P. Carlos, J. L. Fallou, P. Garganne, A. Veyssière, and L. S. Cardman, Phys. Lett. 139B, 254 (1984).

[23]A. Veyssière, H. Beil, R. Bergère, P. Carlos, A. Leprêtre, and K. Kernbath, Nucl. Phys. A199, 45 (1973).

[24]J. T. Caldwell, E. J. Dowdy, B. L. Berman, R. A. Alvarez, and P. Meyer, Phys. Rev. C 21, 1215 (1980); and Los Alamos Report No. LA-UR 76-1615.

[25]W. Wilke, Diploma thesis, University Giessen (1980) (unpublished).

[26]R. Vandenbosch and J. R. Huizenga, *Nuclear Fission* (Academic, New York, 1973).

[27]E. H. Auerbach and F. G. J. Perey, BNL Report No. 765, Brookhaven National Lab., Upton, NY, 1962 (unpublished).

[28]Th. Weber, R. D. Heil, U. Kneissl, W. Wilke, Th. Kihm, K. T. Knöpfle, and H. J. Emrich, Nucl. Phys. A510, 1 (1990); and Th. Weber, Doctoral thesis, University Giessen (1987) (unpublished).

[29]R. Vandenbosch, Phys. Lett. 45B, 207 (1973).

[30]A. H. Wapstra and N. B. Gove, Nucl. Data Tables 9, 265 (1971).

[31]S. Bjørnholm and J. E. Lynn, Rev. Mod. Phys. 52, 725 (1980).

[32]J. Blons, B. Fabbro, C. Mazur, D. Paya, Y. Patin, and M. Ribrag, Nucl. Phys. A477, 231 (1988).

[33]H. Rösler, F. Plasil, and H. W. Schmitt, Phys. Lett. 38B, 501 (1972).

[34]B. D. Wilkins, E. P. Steinberg, and R. R. Chasman, Phys. Rev. C 14, 1832 (1976).

[35]E. Konecny, H. J. Specht, and J. Weber, Phys. Lett. 45B, 329 (1973).

[36]S. Grossmann, U. Brosa, and A. Müller, Nucl. Phys. A482, 340 (1988).

[37]H. H. Knitter, F. J. Hambsch, C. Budtz-Jørgensen, and J. P. Theobald, Z. Naturf. 42a, 786 (1987); and F. J. Hambsch, H. H. Knitter, C. Budtz-Jørgensen, and J. P. Theobald, Nucl. Phys. A491, 56 (1989).

[38]B. M. Gokhberg, L. D. Kozlov, S. K. Lisin, L. N. Morozov, V. A. Pchelin, L. V. Chistyakov, V. A. Shigin, V. M. Shubko, and Yu. A. Yashin, Zh. Eksp. Teor. Fiz. 47, 320 (1988) [Sov. J. Nucl. Phys. 47, 201 (1988)].

[39]Th. Weber, R. D. Heil, U. Kneissl, W. Wilke, H. J. Emrich, Th. Kihm, and K. T. Knöpfle, Phys. Rev. Lett. 62, 129 (1989).

[40]Th. Weber, W. Wilke, H. J. Emrich, R. D. Heil, Th. Kihm, U. Kneissl, K. T. Knöpfle, U. Seemann, F. Steiper, and H. Ströher, Nucl. Phys. A502, 279c (1989).